Low-Aspect-Ratio Toroidal Equilibria of Electron Clouds

Puravi Zaveri, P. I. John, K. Avinash, and P. K. Kaw
Institute for Plasma Research, Bhat, Gandhinagar 382 424, India
(Received 25 June 1991)

Toroidal electron clouds with a low aspect ratio (as small as 1.3) and lasting for thousands of poloidal rotation periods have been formed in the laboratory. Characteristic toroidal effects like a large inward shift of the minor axis of equipotential contours, elliptical and triangular deformations, etc., have been observed experimentally for the first time. The results of new analytic and numerical investigations of low-aspect-ratio electron cloud equilibria, which reproduce many of the observed features, are also presented.

PACS numbers: 52.25.Wz, 52.55.Lf

Non-neutral clouds consisting of charged particles of a single species trapped in simple magnetic bottles have turned out to be excellent test beds for the study of many fundamental properties of confined plasmas. In a series of elegant experiments, Malmberg *et al.* [1] have studied the equilibrium structure, stability, vortex excitation, and transport properties of magnetized cylindrical electron clouds trapped axially by electrostatic potentials. Many collective properties of such non-neutral plasmas in the cylindrical geometry have thus been elucidated. In contrast to electron clouds in linear traps, toroidal electron plasmas—although chronologically first [2]—do not seem to have been studied in depth. Toroidal electron clouds are fundamentally different from cylindrical ones. First, the cloud, being endless, needs no electrostatic potentials along B for confinement. Second, in the single-particle picture, the electrons should simply be lost from the trap due to curvature drifts. However, in contrast to neutral plasmas in a toroidal trap, collective effects due to strong space-charge fields give an $\mathbf{E}\times\mathbf{B}$ rotation to the electron fluid which overcomes curvature drifts and gives confinement without a rotational transform. This may be seen either through a hydrodynamic picture or in terms of adiabatic invariants in a single-particle description [3]. Third, a toroidal electron cloud experiences electrostatic hoop forces which tend to expand the ring. An equilibrium is found by moving closer to the inboard conducting shell, producing image forces to balance the hoop force [4]. The stronger the toroidicity, the greater the shift towards the major axis. A strong inward shift squashing the equipotential surfaces against the inner wall also strongly distorts the surfaces generating large ellipticity and triangularity. Early experiments [2,5], primarily motivated towards the development of heavy-ion accelerators, were done in large-aspect-ratio devices, in which the toroidal effects were not playing any significant role; nor was any systematic attempt made to study these characteristic toroidal effects.

In this Letter, we report the results of a new experiment specifically designed for the detailed study of the equilibrium structure of a fat toroidal electron cloud with an aspect ratio close to unity. The toroidal features of the cloud, such as the inward shift of the minor axis, the strong ellipticity of constant potential surfaces, etc., have been experimentally observed for the first time. We also present results of new analytical and numerical investigations which reproduce many of these observed features.

A schematic diagram of the experimental apparatus is given in Fig. 1. A central conductor A produces the toroidal magnetic field. The vacuum vessel is a toroidal cavity of rectangular cross section with the central hole snugly fitting coaxially around the central conductor. The base pressure is 4×10^{-7} torr. The electron injector is similar to that used by Clark *et al.* [5]. The emission current at 200 V bias and zero magnetic field is 150 mA.

High-impedance potential probes, at various toroidal locations, movable in the poloidal plane and with sufficient frequency response, have been the primary diagnostic in these experiments. These measurements give us a temporal and spatial average picture of the equipotential contours (estimated accuracy of a few percent), which is what is required for equilibrium structure measurements. Wall probes were used in the charge measuring mode by integrating the current flowing into the ground through a 50-Ω resistance.

The wall-probe data are shown in Fig. 2. They show that substantial charge injection takes place for the first 15 μsec only. This is followed by a quiescent period of 30 μsec and finally a high-frequency noise region with fre-

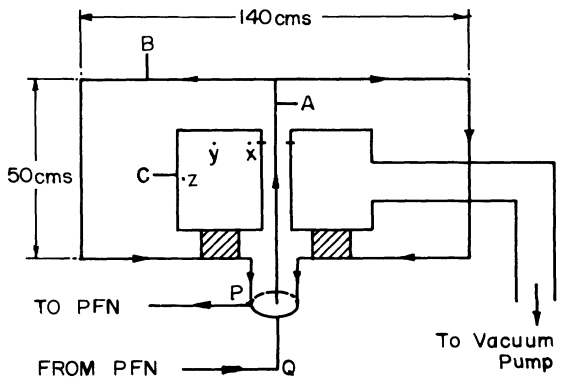

FIG. 1. A vertical cross section of the apparatus. PFN stands for pulse forming network.

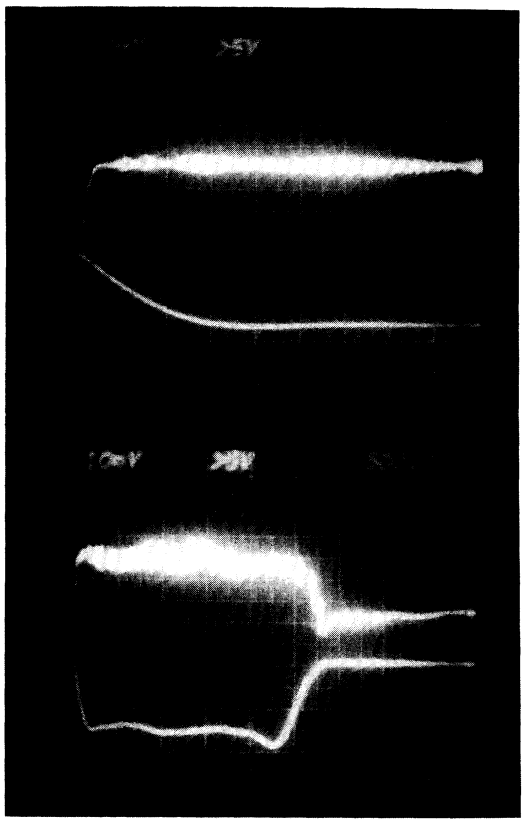

FIG. 2. Wall-probe data: (a) The upper trace shows the charging pulse and the bottom trace is the magnetic field; (b) the upper trace shows the diocotron instability, persisting for the entire magnetic field duration (bottom trace).

quencies between 0.5 and 1 MHz. The total charge confined in the vessel is about 0.3 μC. The potential distribution was measured at a large number of points in the poloidal plane, and equipotential contours plotted [Figs. 3(a) and 3(b)]. These inward clouds have been obtained by injecting electrons from point "x" in Fig. 1. The toroidal symmetry of the clouds is confirmed experimentally using probes at multiple toroidal locations. The aspect ratio achieved in the experiment is about 1.3. The minimum potential point is seen to be located not at the minor axis, but shifted inwards by as much as 4 cm. The equipotential contours are also seen to be strongly elongated in the vertical direction. The clouds last for about 2 to 2.5 msec. The density measurements (made by grounding the probe electronically for 20 μsec) indicate that electron densities are in the range of 10^8 cm^{-3}; this is in reasonable agreement with the wall-probe data of the total charge on the electron cloud. When electrons are injected from the points "y" and "z," the entire cloud is shifted towards the lower far corner of the vacuum vessel [Fig. 3(c)]. As discussed later these strongly displaced locations of equilibria may be related to stray electric fields in the vacuum vessel caused by the bias on the bare cathode.

The following observations indicate that the injection physics is more complex than the usual "inductive charging" scenario: (a) Major injection is completed in the first 15 μsec when B ($\sim$10 G) is less than the Hull [6] cutoff field B_H corresponding to the cathode-anode gap ($B_H \sim 73$ G) but greater than B_H corresponding to the cathode-vessel wall gap ($B_H \sim 3$ G) indicating that an electron current of 20–30 mA going to the vessel wall at $t=0$ contributes to electrons trapped in the cloud. (b) To explain the existence of the cloud for 2–2.5 msec in the presence of charge neutralization ($\tau_i \sim 2$ msec), we must have a continued small injection current (perhaps masked by noise on the probe signal) even after the magnetic field has stopped rising. Daugherty, Eninger, and Janes [2] have also observed these features, although they claim that the injection was entirely due to inductive charging.

We have observed a distinct transition from single-particle to collective behavior. At low emission currents, up to 1 mA, the particles are confined to a region directly connecting the diode and the lower wall, as would be expected if the particles followed curvature drifts. There is no significant potential in this region. When the current exceeds 1 mA, the region occupied by the particles expands radially, the potentials reach values larger than the cathode-anode potential, and the minimum potential region shifts to a radial location away from that of the filament. The Debye length calculated from the particle density obtained using the critical current and the measured temperature of 20 eV is comparable to the chamber dimensions, consistent with the picture of transition to collective behavior at this current. Potential wells with a well depth larger than the anode-cathode voltage indicate an accumulation of electrons within the vessel. The charge injection lasts only 15 μsec whereas the equipotential contours last the duration of the magnetic field, strongly supporting the case for a toroidal equilibrium of the electron cloud. With the ∇B drift velocity of order 6×10^6 cm/sec, it would take electrons only $\sim$3 μsec to reach the chamber wall. The equilibrium arises because the $\mathbf{E}\times\mathbf{B}$ drift in the poloidal direction due to space-charge fields is of order 10^8 cm/sec which is more than an order of magnitude faster. Thus the collective effects dominate over the single-particle drift effects and ensure that the equilibrium lasts for long periods. The equipotential contours are nearly the trajectories for the electron guiding center. The ratio of the Larmor radius to the major radius at the minor axis is 0.03 and the inertial displacement of drift surfaces from equipotential surfaces is 0.6 cm and hence negligible. No significant change in the equilibrium is observed when the magnetic field is varied from 40 to 150 G, indicating that inertial effects are not important.

Since the collective effects are dominant, we may use a hydrodynamic description to explain the special properties of the toroidal equilibrium. In the limit of zero electron inertia and diamagnetism, it has been shown that the two-dimensional equilibrium is governed by an equation

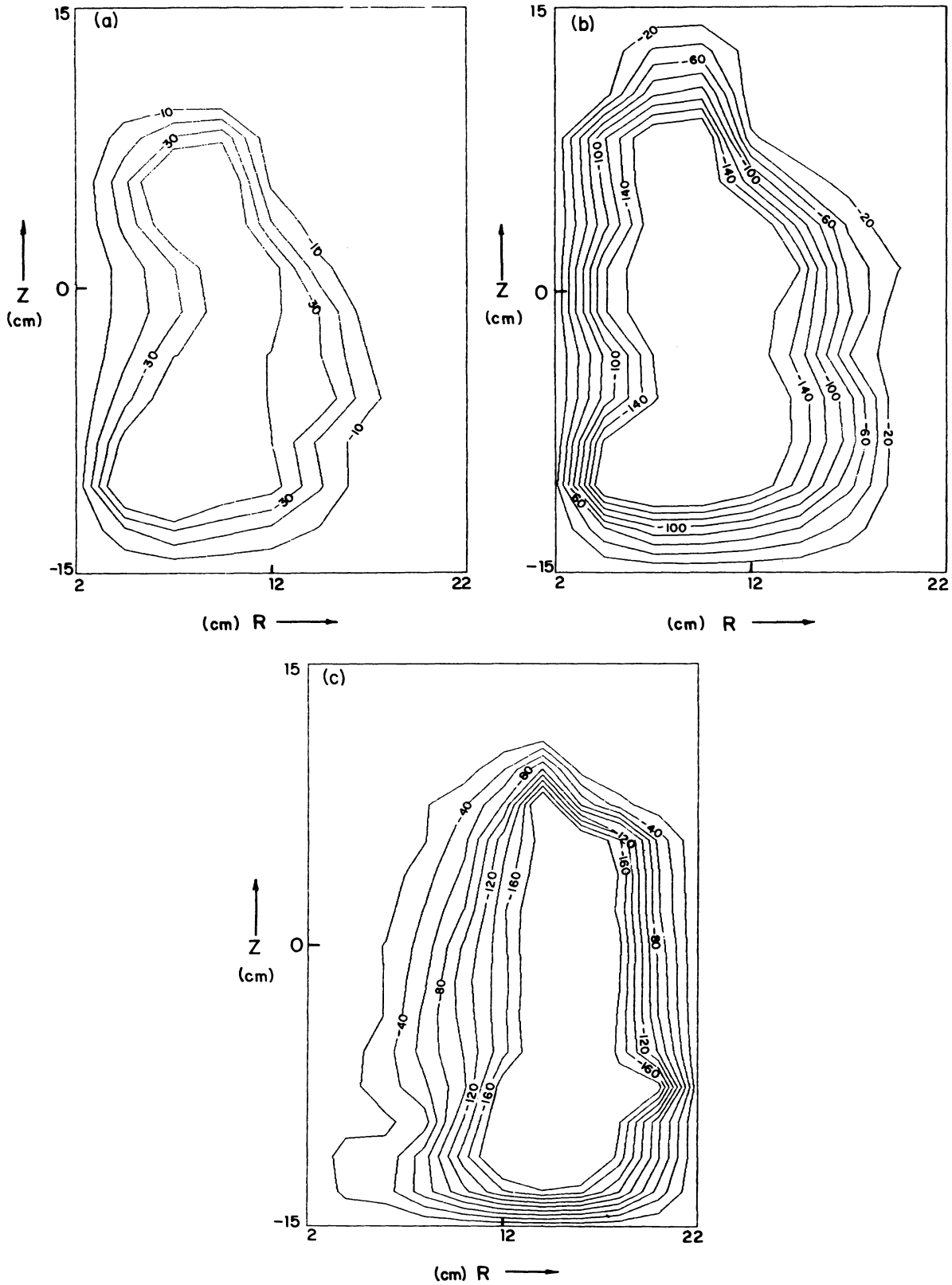

FIG. 3. The contours of equipotentials obtained from the experiments (a) at 100 μsec and (b) at 2 msec; (c) electron cloud located near the outer wall. The numbers on the contours are in volts. The time evolution may be attributed to noncollisional toroidal transport effects. The magnetic field at the potential minimum for (a) and (b) is 60 G, and for (c) it is 120 G.

[3] of the type $\nabla^2\phi = f(\phi)/R^2$, where $f(\phi)$ is an arbitrary function of ϕ. Using this equation the existence of an equilibrium with closed potential and drift surfaces has been demonstrated [4]. In the large-aspect-ratio torus ($\epsilon = a/R_0 \ll 1$), equilibrium consists of circular equipotentials which are displaced towards the major axis by a distance $\delta \sim \epsilon a$. The drift surfaces are also closed and displaced further inwards by a distance $\sim \epsilon q a$ ($q = \omega_p^2/\omega_c^2$). This equilibrium can also be understood in terms of a force balance [4] along $\hat{\mathbf{R}}$. As the aspect ratio is decreased, the normalized shift $\delta/a \to 1$. The strong inward shift for low-aspect-ratio toroids also results in strong distortions, i.e., ellipticity, triangularity, etc. To investigate the low-aspect-ratio toroidal equilibria, we have determined the functional form of $f(\phi)$ by fitting a polynomial to the experimental curve of nR^2 vs ϕ. The best fit is obtained for $f(\phi) = a + b\phi + c\phi^2$ with $a = 23.4$, $b = 0.59$, and $c = 0.006$. Using this form of $f(\phi)$, the equation $\nabla^2\phi = f(\phi)/R^2$ was solved for aspect ratio $\epsilon^{-1} = 1.2$. The results are shown in Fig. 4 where we find that for low aspect ratio, the equipotentials are strongly inward shifted and are elliptic. This is qualitatively consistent with strong inward shift and ellipticity observed in the experimental equipotential of Figs. 3(a) and 3(b). From Fig. 3 the experimentally observed shift is 4 cm from the minor axis and the ellipticity is 2.2, while numerically computed values from Fig. 4 are 6.9 cm and 1.9, respectively. The ellipticities in the two cases are in better agreement than the shifts. The main reason for this discrepancy is the presence of stray fields which are not included in the above calculation but are always present. To get further insight into the importance of this effect, we consider an exact solution with $f(\phi) = \text{const}$. This solution can be written as $\phi = \frac{1}{2}(\ln R)^2 + c_1 + c_2 \ln R + c_3(z^2 - R^2/2)$, where c_1-c_3 are constants. We determine c_2 and c_3 by demanding that the outermost surface passes through $R_{1,2} = R_0 \pm a$, and c_3 can be used to fix the ellipticity of the surface near the axis. By computing the solution for different horizontal fields given by $\phi(R_0 + a) - \phi(R_0 - a) = \phi_1$ we find that fields as low as ~ 2 V (as compared to 200 V of peak potential) can strongly displace the equilibrium determined by self-fields alone. One of the main candidates for stray fields is the bare cathode biased to ~ -200 V. We believe that such stray fields are responsible for the outward shift shown in Fig. 3(c).

To conclude, we have presented the first observations of toroidal effects in low-aspect-ratio electron rings. The strong displacement of the minor axis and elliptic distortions of constant potential surfaces are shown to be consistent with a hydrodynamic theory of the equilibrium which emphasizes collective effects. These charged electron rings have interesting similarities and differences from neutral plasma toroidal current filaments used for confining hot plasmas in thermonuclear research. Capacitance effects replace inductive effects, image charges replace image currents, inward shift replaces outward shift,

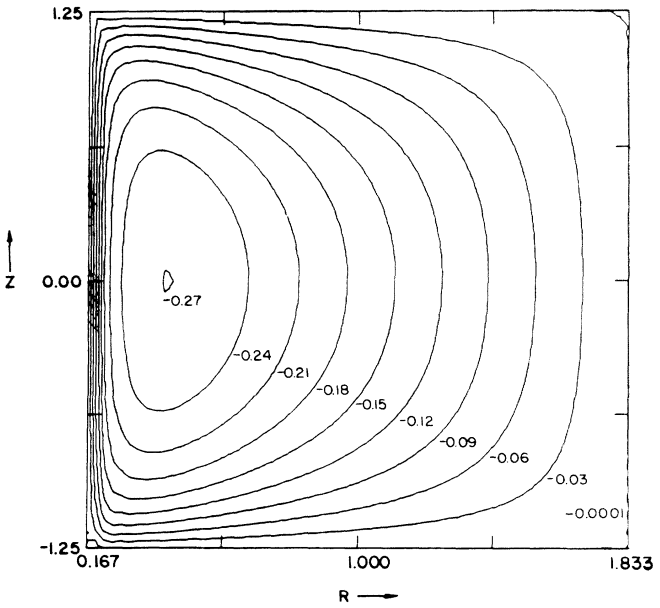

FIG. 4. Numerical solution of $\nabla^2\phi = f(\phi)/R^2$ for $\epsilon^{-1} = 1.2$ and $f(\phi) = a + b\phi + c\phi^2$. The various equipotentials are labeled with ϕ measured in dimensionless units.

dc electric fields take the role of equilibrium vertical magnetic fields, and vortex formation replaces magnetic island formation. In the same way, magnetic field line reconnection of neutral plasmas is replaced by the vortex merger in non-neutral plasmas, while the role of resistivity is played by electron viscosity. Many of these effects remain to be explored yet. Finally a point of contrast from electron cloud experiments in linear traps should be emphasized. The confinement in linear traps is more rugged, being based on exact constants of motion. The toroidal trap confines only through adiabatic invariances which can be broken by various resonant effects. We thus expect to see interesting stochastic [7] transport phenomena in the toroidal experiments.

[1] J. H. Malmberg, C. F. Driscoll, B. Beck, D. L. Eggleston, J. Fajans, K. Fine, X.-P Huang, and A. W. Hyatt, in *Non-Neutral Plasma Physics*, edited by C. Roberson and C. Driscoll, AIP Conf. Proc. No. 175 (AIP, New York, 1988).

[2] J. D. Daugherty, J. E. Eninger, and G. S. Janes, Phys. Fluids **12**, 2677 (1969).

[3] J. D. Daugherty and R. H. Levy, Phys. Fluids **10**, 155 (1967).

[4] K. Avinash, Phys. Fluids B **3**, 3226 (1991).

[5] W. Clark, P. Korn, A. Mondelli, and N. Rostoker, Phys. Rev. Lett. **37**, 592 (1976).

[6] W. A. Hull, Phys. Rev. **18**, 13 (1921).

[7] L. Turner, Phys. Fluids B **3**, 1355 (1991).

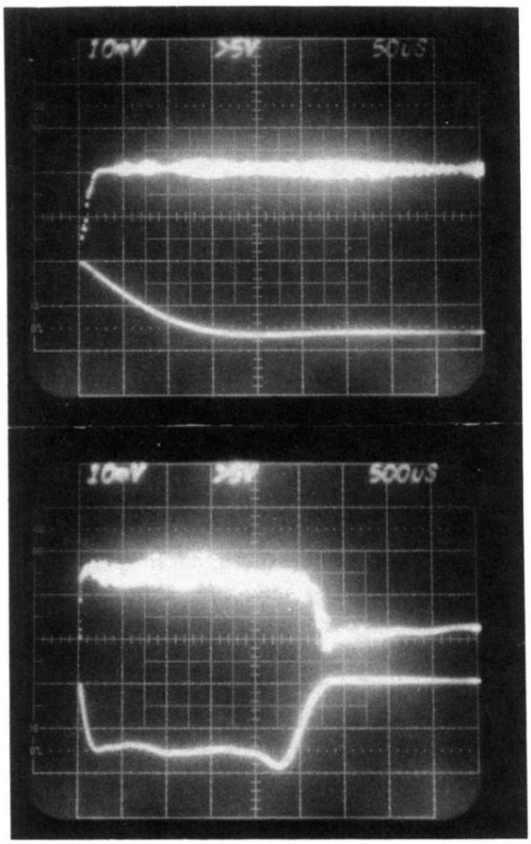

(a)

(b)

FIG. 2. Wall-probe data: (a) The upper trace shows the charging pulse and the bottom trace is the magnetic field; (b) the upper trace shows the diocotron instability, persisting for the entire magnetic field duration (bottom trace).